An Atomic Model for the Pleated β-Sheet Structure of Aβ Amyloid Protofilaments

Leping Li,* Thomas A. Darden,# L. Bartolotti,§ Dorothea Kominos,¶ and Lee G. Pedersen#‖

*Health Effects Laboratory Division, National Institute for Occupational Safety and Health, Morgantown, West Virginia 26505-2845; #National Institute of Environmental Health Sciences, Research Triangle Park, North Carolina 27709; §North Carolina Supercomputing Center, Research Triangle Park, North Carolina 27709; ¶Hoechst Marion Roussel, Somerville, New Jersey 08876; and ‖Department of Chemistry, University of North Carolina, Chapel Hill, North Carolina 27599 USA

ABSTRACT Synchrotron x-ray studies on amyloid fibrils have suggested that the stacked pleated β-sheets are twisted so that a repeating unit of 24 β-strands forms a helical turn around the fibril axis (Sunde et al., 1997. *J. Mol. Biol*. 273:729–739). Based on this morphological study, we have constructed an atomic model for the twisted pleated β-sheet of human Aβ amyloid protofilament. In the model, 48 monomers of Aβ 12–42 stack (four per layer) to form a helical turn of β-sheet. Each monomer is in an antiparallel β-sheet conformation with a turn located at residues 25–28. Residues 17–21 and 31–36 form a hydrophobic core along the fibril axis. The hydrophobic core should play a critical role in initializing Aβ aggregation and in stabilizing the aggregates. The model was tested using molecular dynamics simulations in explicit aqueous solution, with the particle mesh Ewald (PME) method employed to accommodate long-range electrostatic forces. Based on the molecular dynamics simulations, we hypothesize that an isolated protofilament, if it exists, may not be twisted, as it appears to be when in the fibril environment. The twisted nature of the protofilaments in amyloid fibrils is likely the result of stabilizing packing interactions of the protofilaments. The model also provides a binding mode for Congo red on Aβ amyloid fibrils. The model may be useful for the design of Aβ aggregation inhibitors.

INTRODUCTION

The hallmark of Alzheimer's disease (AD) is the extracellular deposition of senile plaques and intraceullar neurofibrillary tangles (Glenner and Wong, 1984). The principal component of the amyloid plaques is a 39–43-amino acid peptide (Aβ) derived from a much larger protein called amyloid β-protein precursor (AβPP) (Kang et al., 1987). Although the physiological functions of the Aβ peptides are still under investigation, it is widely believed that Aβ plays an important role in the pathogenesis of AD (see Selkoe, 1996, for a review). The conformation of Aβ is environment-dependent. In aqueous solution, Aβ exists mainly as a random coil. However, in helix-promoting solvents such as trifluoroacetic acid (TFA) or in a lipid environment, Aβ adopts an α-helical conformation (Sticht et al., 1995; Coles et al., 1998). Aβ can show two helical regions connected by a hinge around residues 24–28 or a single α-helix in low dielectric environments (Sticht et al., 1995; Coles et al., 1998). It has been suggested that Aβ is not toxic in a nonaggregate form, but becomes detrimental after undergoing a structural transition from a random coil to a β-sheet conformation followed by fibril formation (Pike et al., 1991; Burgevin et al. 1994; Lorenzo and Yankner, 1994; Simmons et al., 1994). Because the C-terminal residues of Aβ are hydrophobic, the longer Aβ peptides (1–42 and -43) aggregate more rapidly than the shorter forms under physiological conditions. The longer peptides may also seed amyloid fibril formation in vivo (Jarrett et al., 1993). Kinetic studies have shown that polymerization is a two-step process (nucleation and elongation), of which the nucleation event is the rate-limiting step (Jarrett et al., 1993; Lomakin et al., 1996; Harper et al., 1997). In a study of temperature-dependent Aβ fibril formation, Kusumoto et al. proposed that a large activation energy is required to add a monomer to the growing fibril tip. The process may involve a significant increase in entropy, suggesting that a large conformational change is required for Aβ (Kusumoto et al., 1998). This result is consistent with the conclusion that the conformation of Aβ in solution is different from that in the fibrils and that a conformational change is needed for Aβ to polymerize. Aβ may exist as a metastable conformation in aqueous solution (Lee et al., 1995) under conditions in which Aβ can aggregate. Perhaps, through hydrophobic collapse (Dill, 1990) with concomitant conformational changes, Aβ may form a dimer, a tetramer, and a higher ordered species (Walsh et al., 1997).

Because of the insoluble and noncrystalline nature of the fibrils, experimental studies on the structures of amyloid fibrils have been limited mainly to low-angle x-ray fibril diffraction and solid-state NMR. Although the details of the structures of amyloid fibrils remain elusive, these studies have suggested that amyloid fibrils contain a similar structural core—the pleated β-sheet or so-called cross-β-structure, irrespective of the nature and sources of amyloid proteins/peptides (Inouye et al., 1993; Lansbury et al., 1995; Sunde et al., 1997). The widely adopted model for the cross-β structure is the one proposed by Pauling (Pauling and Corey, 1951). In the model, the β-strands are perpen-

Received for publication 14 December 1998 and in final form 26 March 1999.

Address reprint requests to Dr. Lee G. Pedersen, Department of Chemistry, CB# 3290, University of North Carolina at Chapel Hill, Chapel Hill, NC 27599-3290. Tel.: 919-962-1578; Fax: 919-962-2388; E-mail: pedersen@niehs.nih.gov.

0006-3495/99/06/2871/08 $2.00

dicular to the fibril axis that runs parallel to the direction of the backbone hydrogen bonds. The interstrand and intersheet distances are ~4.7 and ~10.0 Å (Fraser et al., 1991; Inouye et al., 1993; Blake and Serpell, 1996), respectively. The pleated β-sheet structure is the core of the protofilaments in amyloid fibrils. High-resolution electron microscopy studies suggested that amyloid fibrils are composed of three to six such protofilaments (Kirschner et al., 1987; Fraser et al., 1991; Inouye et al., 1993; Serpell et al., 1995; Malinchik et al., 1998). Although Pauling's pleated β-sheet model may have captured the essence of the core structure of the protofilament, solid-state NMR studies have revealed that the pleated β-sheets are not perfectly stacked (Lansbury, 1992), as required in Pauling's model (Pauling and Corey, 1951). Consistent with this idea, analysis of recent synchrotron x-ray fibril diffraction data from transthyretin (TTR) amyloid fibrils led to the conclusion that the pleated β-sheets are twisted, for which a 24 β-stranded unit, with its β-strands arranged perpendicular to the fibril axis, forms a complete helical turn (Blake and Serpell, 1995). This conclusion was confirmed later based on synchrotron x-ray studies on eight different amyloid fibrils (Sunde et al., 1997). The length of the pleated β-sheet for a complete turn is ~115 Å (Blake and Serpell, 1996; Sunde et al., 1997).

Although atomic details of the structure of the presumed Aβ pleated β-sheet remain unknown, experimental studies suggest that Aβ may form an antiparallel β-sheet with a turn located around residues 26–29 (Ser-Asn-Lys-Gly) (Hilbich et al., 1991). The region of Aβ proposed as a turn in Aβ amyloid fibrils also shows a turn-like motif in solution (see a summary in Coles et al., 1998). Such a turn would facilitate the alignment of the hydrophobic residues Leu^{17}-Val^{18}-Phe^{19}-Phe^{20}-Ala^{21} in one strand with residues Gly^{38}-Gly^{37}-Val^{36}-Met^{35}-Leu^{34} in another strand. However, by shifting the turn one residue back toward the N-terminus to 25–28 (Gly-Ser-Asn-Lys), residues 17–21 would pair with residues Val^{36}-Met^{35}-Leu^{34}-Gly^{33}-Ile^{32}. This turn arrangement eliminates the two glycine residues (Gly^{37} and Gly^{38}) as core residues of the antiparallel β-sheet. In fact, the contacts between residues Leu^{17}-Phe^{20} and Ile^{31}-Met^{35} in solution have been detected when Aβ is in a plaque competent form (Lee et al., 1995). Based on this structural information, we have constructed an antiparallel β-sheet with a turn (type I) located at residues 25–28 for Aβ 12–42. The N-terminal residues 1–11 were not included, because the structure of these residues is less defined and their role in Aβ amyloid fibril formation, if any, is not known. The N-terminus of the Aβ 12–42 peptide model was blocked by an acetyl group, whereas the C-terminus remained charged. The antiparallel β-sheets were then stacked to form a twisted pleated β-sheet according to the model proposed by Blake (Blake and Serpell, 1996; Sunde et al., 1997). The model was then tested using molecular dynamics simulations in explicit solvent. The particle mesh Ewald (PME) method (Darden et al., 1993) was employed to properly accommodate long-range electrostatic forces. Herein we report the basic features of the solvated and equilibrated atomic model for the pleated β-sheet.

MATERIALS AND METHODS

Model construction

The high-resolution crystal structure of TTR (pdb entry 2pab) was used as the starting point for construction of the basic building block, a dimer of an antiparallel β-sheet. Like Aβ, TTR has been implicated in senile systemic amyloidosis, as well as other familial amyloidotic polyneuropathy (Kelly, 1998). The crystal structure was solved at 1.8-Å resolution (Blake et al., 1978). In the x-ray crystal structure of the TTR dimer, residues 105–112 and 114–121 from each monomer form an antiparallel β-sheet at the dimer interface. The two sheets (four strands) are also in an antiparallel arrangement. Using the coordinates of the two sheets in TTR, we built, by side-chain replacement, a dimer of Aβ 12–42. The original turn (type I) at residues 112–115 in TTR was used to model the turn for residues 25–28 in Aβ 12–42. The strands from TTR were extended at both N- and C-termini to fill out the human Aβ length in such a way that the remaining residues were in an antiparallel β-sheet. The sheets were then realigned (translated) to obtain maximal hydrogen bonding (a total of 14 hydrogen bonds) between the sheets (Fig. 1). The distance (Cα-Cα) between two adjacent strands was 4.7 Å. The dimer was then translated three times in a direction perpendicular to the plane defined by the Cα atoms of the dimer, each by 9.7 Å relative to its immediate Cα plane. That resulted in a 8-mer. A 16-mer was created by stacking another 8-mer on the top of the 8-mer in a direction parallel to the direction of the backbone hydrogen bonds. The distance between the two 8-mers was 4.7 Å. A schematic diagram for the construction process is shown in Fig. 2. The stacking was continued along the fibril axis to give a 48-mer. To construct the twisted pleated β-sheet, each of the four-monomer units on the same level (above) relative to the fibril axis was rotated by 15° with respect to its immediate neighbor (below) around the fibril axis. In the final twisted β-pleated sheet model, there are 48 monomers of Aβ 12–42 (96 strands) (Fig. 3). The height of the pleated β-sheet is ~115 Å, which is consistent with the length of the repeat unit reported from the synchrotron x-ray studies (Blake and Serpell, 1996; Sunde et al., 1997). Surprisingly, there were few steric clashes in the complex. All of the close contacts in the initial model involved side-chain atoms and were uneventfully removed by energy minimization. The model was then solvated and subject to a molecular dynamics simulation for 600 ps. The initial twist imposed in the starting structure appeared to decrease during the simulation. Some of the lost backbone hydrogen bonds between two adjacent layers due to the twist recovered (see Results and Discussion).

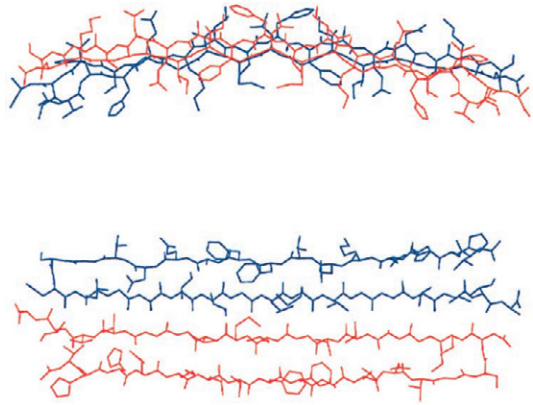

FIGURE 1 Atomic model of the starting antiparallel β-sheet dimer. For clarity, hydrogen atoms were omitted. One monomer is in red, and the other is in blue. (*A*) Top view along the backbone hydrogen bond direction. (*B*) Side view orthogonal to the plane defined by the backbone hydrogen bonds.

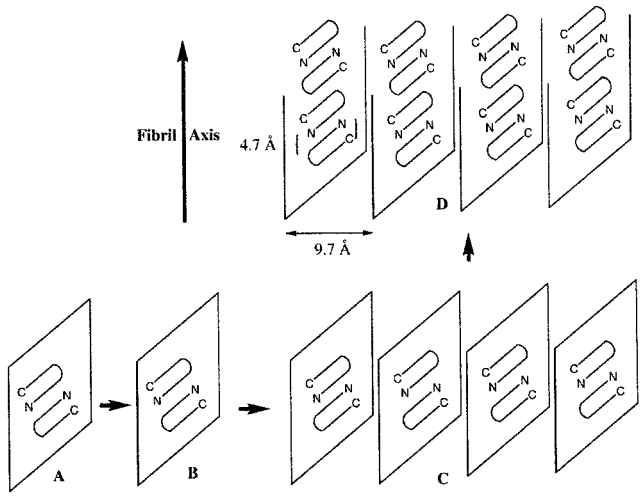

FIGURE 2 A schematic diagram for the construction process for the perfectly stacked 16-mer. (*A*) A four-strand antiparallel β-sheet unit from the dimer interface of the crystal structure of TTR (pdb entry 2pab) (residues 105–112 and 114–121). (*B*) A dimer of Aβ 12–42 in an antiparallel β-sheet conformation. There are 14 hydrogen bonds between two adjacent strands (both intra- and intermonomer). This distance between any two adjacent strands is ~4.7 Å. (*C*) The dimer is translated three times in a direction perpendicular to the plane defined by the Cα atoms of the dimer, each by ~9.7 Å. An 8-mer results. (*D*) A perfectly stacked 16-mer. It was constructed by stacking (parallel) two 8-mers together in the direction of the fibril axis.

We reasoned that a perfectly stacked structure would be more stable and could be a better model for an isolated Aβ protofilament. As a control, a parallel simulation was also performed on an untwisted 16-mer for 2.5 ns.

Molecular dynamics simulations

The molecular dynamics simulations were performed according to procedures reported previously (Li et al., 1997). Briefly, the simulations were performed using the Amber 4.1 package, with the PME method (Darden et al., 1993) employed to accommodate long-range electrostatic forces. The simulations utilized Amber all-atom force field (Cornell et al., 1995) with a step size of 2 fs. Nonbonded interactions were updated every step. All covalent bonds involving hydrogen atoms were constrained using a modified SHAKE (Hamaguchi et al., 1992). Initially, the protein was solvated in a large box of Monte Carlo TIP3P water. The numbers of water molecules used were ~9,000 and ~24,000 for the 16-mer and 48-mer, respectively. Because each monomer carries one negative net charge, 16 and 48 Na^+ ions were needed to neutralize the system for the 16-mer and the 48-mer, respectively. The counterions were placed at least 10 Å from the peptide atoms and from each other. The ions and water were then energy minimized for 100 steps, followed by equilibration for 100 ps. The ions and water were then reminimized, followed by minimization of the whole system. The system was then slowly heated to 300 K within 10 ps at constant volume, while a large Cartesian constraint of 100 kcal/mol · A^2 was placed (temporarily) on the backbone atoms of the peptide monomers. The simulation was continued for another 90 ps. Next, the Cartesian constraint on the backbone atoms was replaced by a (temporary) distance constraint on the backbone hydrogen bonds. For the 16-mer, all of the backbone hydrogen bond (both intra- and interstrand) distances were constrained (temporarily), whereas only the distances between the two strands within a monomer were constrained for the 48-mer. Each simulation was carried out for 200 ps at constant pressure. The constraint on the hydrogen bond distances between monomers in the 16-mer was then removed, with only the constraint on the intramonomer hydrogen bonds remaining. Each simulation was continued for 100 ps. Finally, additional totally unconstrained simulations were carried for 2100 and 300 ps for the 16-mer and the 48-mer, respectively.

RESULTS AND DISCUSSION

Structural features of the Aβ pleated β-sheet model

The model of one helical turn of the twisted pleated β-sheet is composed of 48 monomers of Aβ 12–42. Each monomer contains an antiparallel β-sheet. Overall, there are 96 β-strands. Four strands form a unit and 24 units stack together along the fibril axis. If each unit were twisted by 15° relative to its immediate neighbors (above and below) in the same way, 24 units would make a complete helical turn, with the helical axis parallel to the fibril axis. Because the structure of the monomeric form of Aβ 12–42 was constructed using the structure information of TTR (see methods), the twist angle between the two β-strands in each monomer is not exactly 15°. Given that the angle between the two immediate strands from two different monomers was set at 15°, the helical twist formed by the 24 units in the model was actually nearly a complete turn (~350°).

We note that the four strands in each unit layer are in an identical orientation, and those between two adjacent (above, below) unit layers are in an antiparallel arrangement. In other words, the unit layers stack in an antiparallel fashion. The distance between the two adjacent strands in different unit layers and that between two strands within an unit layer are ~4.7 and ~9.7 Å, respectively (Fig. 2). These distances are consistent with results from x-ray fibril diffraction studies on amyloid fibrils (Fraser et al., 1991; Inouye et al., 1993; Serpell et al., 1995; Sunde et al., 1997; Malinchik et al., 1998).

Within each monomer, residues 17–21 and 31–36 form the core of the antiparallel β-sheet. These residues are hydrophobic. The side chains of these residues pack so as to optimize space filling interactions between monomers in the same unit layer and between monomers in the adjacent unit layers. For example, the side chains of Leu^{17}, Phe^{19}, Ile^{32}, and Val^{36} from one monomer interact with those of Val^{18}, Phe^{20}, Ile^{31}, and Met^{35} from the adjacent monomer in the same unit layer, respectively. The side chains also contact those in the adjacent units, so that a hydrophobic core is formed along the center of the pleated β-sheet (Fig. 4). While the center of the hydrophobic core is totally buried, the edges are solvent exposed. Because hydrophobicity plays an important role in amyloid fibril formation (Jarrett et al., 1993), the buried hydrophobic core could be critical in initializing Aβ aggregation and in fibril elongation. It has been shown, for instance, that substitution of Phe^{19} by a proline residue in Aβ 1–40 abolishes Aβ aggregation, whereas replacing Ala^{21} by a glycine residue decreases the rate of aggregation (Walsh et al., 1997). Double substitutions of Ile for Phe^{19} and Gly for Phe^{20} abolishes fibril formation of Aβ 10–23 (Hilbich et al., 1991). Proline

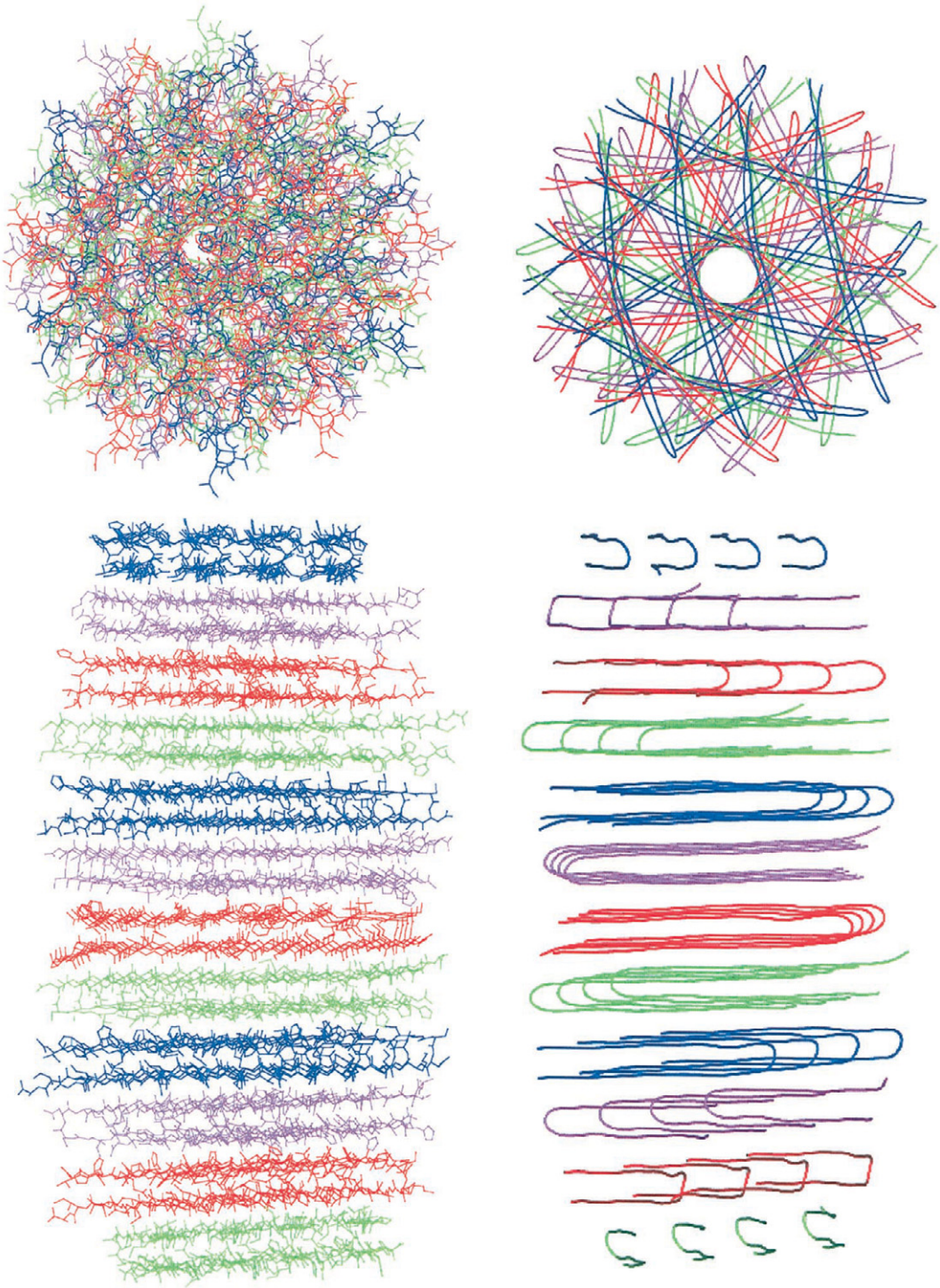

FIGURE 3 The all-heavy atom model of the pleated β-sheet as the core of Aβ amyloid protofilament. The model contains 48 monomers of Aβ 12–42 (96 strands) with four monomers on the same level relative to the fibril axis. Those four monomers are in the same orientation. Each of the four-monomer units is in an antiparallel arrangement with respect to its adjacent unit. The angle between two adjacent units is 15°. (*A*) Top view normal to the fibril axis (all-heavy atom model, *top right*; worm diagram, *top left*). (*B*) Side view along the fibril axis (all-heavy atom model, *bottom left*; worm diagram, *bottom right*).

mutagenesis studies showed that proline replacement of any residues between residues 17–23 of Aβ 12–26 leads to the loss of fibril formation (Wood et al., 1995). In a study of the aggregation of Aβ 25–35, Pike et al. concluded that residues 29–35 are important for Aβ aggregation (Pike et al., 1995). Likewise, the C-terminal hydrophobic residues are of importance in Aβ aggregation and seeding (Jarrett et al., 1993). It has been shown, for instance, that a pentapeptide

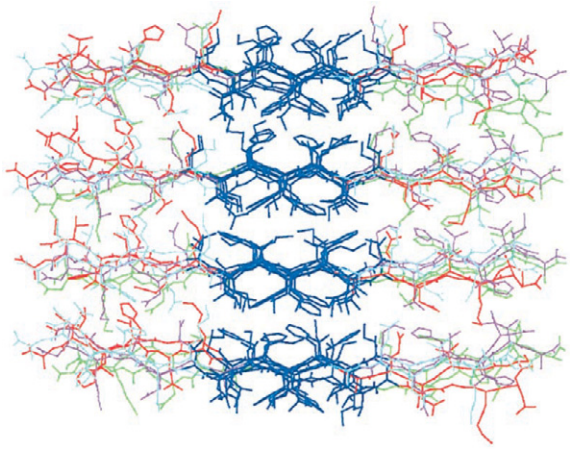

FIGURE 4 Hydrophobic core formed by the side-chain atoms of residues 17–21 and 31–36 along the fibril axis in the average structure of the 16-mer generated from the coordinates of a simulation period of 1200–2000 ps. For clarity, hydrogen atoms were omitted. Different layers are in different colors (viewed along the fibril axis, parallel to the backbone hydrogen bond direction). The hydrophobic core is in blue.

consisting of Aβ 16–20 can bind to Aβ 1–40 and prevent its aggregation (Tjernberg et al., 1996). Interestingly, the contacts between these hydrophobic residues (residues 17–20 and 31–35) in our pleated β-sheet model were detected for Aβ 10–35 when it was in a plaque competent conformation (Lee et al. 1995). Whereas the buried hydrophobic core could be critical in the formation of the protofilament, the exposed fraction could play an important role in assembling the protofilaments into fibrils. Electron microscopy studies have shown that amyloid fibrils consist of three to six protofilaments (Kirschner et al., 1987; Fraser et al., 1991; Inouye et al., 1993; Serpell et al., 1995; Malinchik et al., 1998). It is possible that the exposed hydrophobic residues could be involved in helical packing among the protofilaments. It is known, for instance, that side-chain packing plays an important role in stabilizing helical coiled-coil bundles (Chou et al., 1988; Betz et al., 1997; Langosch and Heringa, 1998).

While the center of our pleated β-sheet structure is hydrophobic, the ends of the sheets are somewhat hydrophilic. Ionic interactions and/or hydrogen bond interactions as additional forces stabilizing the cross-β structure have been proposed (Kirschner et al., 1987; Fraser et al., 1991; Lee et al., 1995). Consistent with those suggestions, the fully solvated and equilibrated untwisted pleated β-sheet model (16-mer, *D* in Fig. 2 and Fig. 4) shows that several polar side chains are involved in intersheet and interlayer electrostatic interactions. For instance, the side chain of Lys^{16} from one monomer interacts with that of Gln^{15} from another monomer in the same unit layer, and that of Glu^{22} and the backbone oxygen atom of Glu^{22} from different monomers in the adjacent unit layer. Likewise, the side chain of Lys^{28} from one unit layer forms interlayer hydrogen bonds with the backbone atoms of Gly^{25} and/or Lys^{28} in the adjacent unit layer.

Molecular dynamics simulations

Two molecular dynamics simulations have been performed, one for the untwisted 16-mer and one for the twisted 48-mer. Both simulations were performed in explicit aqueous solution, with the PME method (Darden et al., 1993) employed to accommodate long-range electrostatic forces. The simulation on the 16-mer was 2.5 ns in length, whereas that on the 48-mer was 600 ps. The 16-mer (untwisted) quickly reached equilibration and remained stabilized during the course of the simulation (Fig. 5 *A*). The root mean square deviation (rmsd) of the backbone atoms of the average structure compared to those of the starting structure is ~2.4 Å. Almost all of the hydrogen bonds between the two antiparallel strands in each monomer as well as those between two adjacent layers remained. The contacts between the side chains of adjacent monomers remained intact. Overall, each monomer remained in an antiparallel conformation, and the structure remained packed through contacts between the adjacent monomers and layers. No significant structural changes occurred during the course of the 2.5-ns simulation. The 48-mer simulation was more problematic and at 600 ps had not stabilized completely (Fig. 5 *B*). Like the 16-mer, each monomer remained in an antiparallel β-sheet conformation. Although the structure remained intact and packed, the 15° twist imposed in the starting structure appeared to lessen during the course of the simulation, particularly in the early stages. It appears that the initially imposed helical twist untwisted in a direction opposite the initial twist, and some of the hydrogen bonding between two adjacent strands from different monomers initially lost to create the twist was recovered. This untwisting may account for the observation that although each monomer remained in an antiparallel β-sheet conformation with an overall complex intact, the rmsd of the backbone atoms

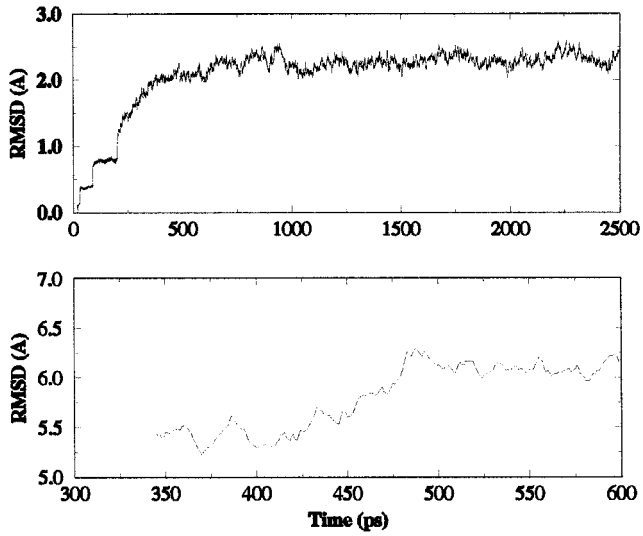

FIGURE 5 Root mean square deviation of the backbone atoms of the 16-mer (*top*) and the 48-mer (*bottom*) relative to the starting structure as a function of the simulation time.

compared to those of the starting structure was relatively large. X-ray diffraction studies on amyloid fibrils have suggested that amyloid fibrils may be composed of three to six protofilaments (Kirschner et al., 1987; Fraser et al., 1991; Inouye et al., 1993; Serpell et al., 1995; Malinchik et al., 1998). The cross-β structure is the core of the protofilament. Thus it is possible that the observed helical nature of the pleated β-sheet may be the result of the packing of protofilaments. It is known that side-chain packing plays an important role in stabilizing the helical bundles (Chou et al., 1988; Betz et al., 1997; Langosch and Heringa, 1998). In a perfectly stacked pleated β-sheet structure, the hydrogen bonding between any two adjacent strands is preserved (Fig. 2). Introduction of a twist into the pleated β-sheet would disrupt some of the hydrogen bonding. However, the loss of the hydrogen bonding could be offset by the gain from the packing interactions among the side chains of the protofilaments. Such a packing would also minimize the overall exposed hydrophobic surface. Therefore, one would assume that an isolated protofilament, if such exists, may not be twisted as seen in amyloid fibrils. And the helical twist of the protofilaments in amyloid fibrils may be the result of dominant packing interactions between the protofilaments. If such is the case, the untwisting of the 48-mer seen during the molecular dynamics simulation would not be surprising. Thus the untwisted 16-mer may be a better model for an isolated pleated β-sheet. Nonetheless, the twisted 48-mer model provides useful information about the core of the pleated β-sheet in amyloid fibrils.

Although the 16-mer reached equilibration, the time scale is too short for an adequate sampling of a system this size. It is not clear if a "local" or a "global" minimum was sampled. To find out, a much longer simulation (in the order of 100 ns to milliseconds) is needed, which is impractical at present. Thus, although the current MD result supports the model, it does not necessarily prove it.

Interactions with Congo red

Congo red has commonly been used to diagnose amyloid deposits (Puchtler et al., 1962). The dye binds to amyloid fibrils, and the fibrils display an intense green birefringence under polarized light. This response is believed to be dependent on the cross-β conformation of the fibrils (DeLellis et al., 1968). In vitro studies have shown that Congo red can inhibit the neurotoxicity of Aβ (Burgevin et al., 1994; Lorenzo and Yankner, 1994). Congo red has also been shown to inhibit Scapie infectivity of prion (Caughey et al., 1993), as well as the pancreatic islet cell toxicity of diabetes-associated amylin (Lorenzo and Yankner, 1994). The ability of Congo red to interact with amyloid fibrils and to possibly inhibit fibril formation has promoted studies on the mechanism by which Congo red interacts with fibrils and on developing Congo red analogs as potential therapeutics. The crystal structure of the insulin dimer/Congo red complex revealed that Congo red intercalated at the dimer interface formed by two β-strands, one from each monomer. The intercalation disrupted the main-chain hydrogen bonds between the two β-strands. This binding mode of Congo red was suggested to be general to all amyloid proteins (Turnell and Finch, 1992). A similar binding mode (Carter and Chou, 1998) was recently proposed for Congo red on Aβ fibrils, based on the insulin/Congo red crystal structure. Although it is possible that Congo red could be sandwiched by two Aβ peptides in solution as aggregation occurs, it is unlikely that it can be intercalated in fibrils that are already formed. Therefore, it is reasonable to assume the interaction between Congo red and amyloid fibrils occurs on the surface of the building fibrils. Examination of the pleated β-sheet model showed that the Cα-Cα distance between Lys^{16} in one monomer and Lys^{16} in an adjacent monomer is 20.8 Å. The distance is similar to that between the two sulfonate groups in Congo red (19.6 Å). The two lysine residues are separated by the hydrophobic residues (residues 17–21), and the two sulfonate groups are linked by a biphenyl group. Thus it is reasonable that Congo red could bind to the surface of amyloid fibrils, with the two sulfonate groups forming salt bridges with the two Lys residues, while the central biphenyl group of Congo red interacts with hydrophobic side chains of residues 17–21 (Fig. 6). In this binding mode, the long axis of Congo red is orthogonal to, rather than parallel to, the fibril axis as proposed (Cooper, 1974; Klunk et al., 1989). Based on this binding model, Congo red would affect the formation of protofilaments by interrupting the packing of the β-sheets, thus preventing fibril formation. This proposed binding mode for Congo red could also be applied to the highly sulfated glycosaminoglycans (HSPG), which have been found to be associated with amyloid fibrils (Snow et al., 1994). In vitro studies have shown that Congo red and HSPG compete for binding site(s) on amyloid fibrils (Pollack et al., 1995).

Comparison with other models

Recently, several models for Aβ amyloid fibrils have been proposed (Lansbury et al., 1995; Benzinger et al., 1998; Chaney et al., 1998; Lazo and Downing, 1998; Mager,

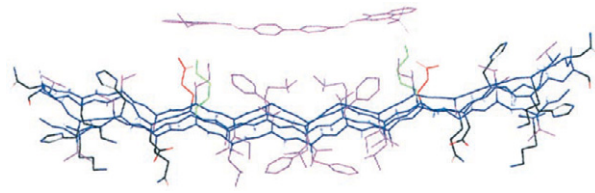

FIGURE 6 A binding mode for Congo red on Aβ amyloid fibrils (same view as in Fig. 1 *A*). The initial structure of the antiparallel dimer was used for Congo red docking. For clarity, only an Aβ dimer and Congo red are shown. Backbone atoms are in blue. Congo red and the hydrophobic core are in magenta. The two Lys residues (Lys^{16} in one monomer and Lys^{16} in another monomer) are in green. The Cα-Cα distance between the two lysine residues in the average structure of the 16-mer remained nearly unchanged compared to that in the starting structure.

1998). These models differ at both the secondary and tertiary structure levels. In the model by Chaney et al., residues 30–42 from one monomer form an antiparallel β-sheet with the same residues from another monomer (Chaney et al., 1998). Accordingly, two-thirds of the Aβ residues are not directly involved in constituting the core of the protofilament, the pleated β-sheet. In the model of Lazo and Downing, the structure of the protofilaments of the amyloid fibrils is represented as a β-helix, with no detailed structural information about the helix presented (Lazo and Downing, 1998). Two other models are based on solid-state NMR studies on Aβ 34–42 (Lansbury et al., 1995) and 10–35 (Benzinger et al., 1998) amyloid fibrils, respectively. Whereas one model suggests that the strands in the pleated β-sheet are in an antiparallel arrangement (Lansbury et al., 1995), the other concludes that the strands are arranged in a parallel fashion (Benzinger et al., 1998). Although it is clear that the amyloid fibrils comprise a structural superfamily and share a common structural feature—the pleated β-sheet—irrespective of the nature of the proteins/peptides (Sunde et al., 1997), it is not clear whether fragments of amyloid precursor proteins/peptides bind in the same way as their full-length counterparts. As further structural studies are conducted with high-resolution techniques, the issue should be resolved. Finally, the very recent model of Mager for Aβ 1–42, which is based on an NMR structure (Sticht et al., 1995) and molecular modeling, has an apolar α-helix (Lys^{16}-Ala^{21}) and an apolar β-strand (Lys^{28}-Val^{40}), the later of which is envisioned to interact in an antiparallel fashion with other strands to form polymers (Mager, 1998). The pleated β-sheet structure of Sunde et al. (1997) is not modeled. Nonetheless, we believe that our model is the first atomic model for the core of the pleated β-sheet of Aβ 1–42 amyloid fibrils. The model is consistent with the morphological model by Blake (Blake and Serpell, 1996; Sunde et al., 1997). The coordinates of the structures presented herein are available on request from the authors.

In conclusion, we have built an atomic model for the core of the pleated β-sheet of Aβ amyloid fibril based on the analysis of synchrotron x-ray diffraction studies on amyloid fibrils (Blake and Serpell, 1995; Sunde et al., 1997), as well as other experimental observations. The model contains 48 monomers of Aβ 12–42. Each monomer is in an antiparallel β-sheet conformation with a turn (type I) located at residues 25–28. Residues 17–21 and 31–36 form a hydrophobic core at the center of the protofilament along the fibril axis. The hydrophobic core may play an important role both in the formation of protofilaments and in the assembly of the protofilaments into amyloid fibrils. The pleated β-sheet of the core of an isolated protofilament, if such exists, may not be twisted, as it apparently is in fibrils. The model also provides a binding mode for Congo red and HSPG on Aβ amyloid fibrils. The model should provide useful insight into the structure of the protofilaments in amyloid fibrils and may be helpful in inhibitor design studies.

We acknowledge the computational resources provided by the North Carolina Supercomputing Center, the Pittsburgh Supercomputing Center, the National Institute of Health-sponsored Computational Structural Biology Resource in Biochemistry at UNC, Chapel Hill and NIH HL-06350. We also acknowledge an anonymous reviewer for constructive suggestions.

REFERENCES

Benzinger, T. L. S., D. M. Gregory, T. S. Burkoth, H. Miller-Auer, D. G. Lynn, R. E. Botto, and S. C. Meredith. 1998. Propagating structure of Alzheimer's β-amyloid (10–35) is parallel β-sheet with residues in exact register. *Proc. Natl. Acad. Sci. USA.* 95:13407–13412.

Betz, S. F., P. A. Liebman, and W. F. DeGrado. 1997. De novo design of native proteins: characterization of proteins intended to fold into antiparallel, rod-like, four-helix bundles. *Biochemistry.* 36:2450–2458.

Blake, C. C., M. J. Geisow, S. J. Oatley, B. Rerat, and C. Rerat. 1978. Structure of prealbumin: secondary, tertiary and quaternary interactions determined by Fourier refinement at 1.8 Å. *J. Mol. Biol.* 121:339–356.

Blake, C., and L. Serpell. 1996. Synchrotron x-ray studies suggest that the core of the transthyretin amyloid fibril is a continuous β-sheet helix. *Structure.* 4:989–998.

Burgevin, M. C., M. Passat, N. Daniel, M. Capet, and A. Doble. 1994. Congo red protects against toxicity of β-amyloid peptides on rat hippocampal neurones. *Neuroreport.* 5:2429–2432.

Carter, D. B., and K. C. Chou. 1998. A model for structure-dependent binding of Congo red to Alzheimer β-amyloid fibrils. *Neurobiol. Aging.* 19:37–44.

Caughey, B., D. Ernst, and R. E. Race. 1993. Congo red inhibition of scrapie agent replication. *J. Virol.* 67:6270–6272.

Chaney, M. O., S. D. Webster, Y. M. Kuo, and A. E. Roher. 1998. Molecular modeling of the Aβ1–42 peptide from Alzheimer's disease. *Protein Eng.* 11:761–767.

Chou, K. C., G. M. Maggiora, G. Nemethy, and H. A. Scheraga. 1988. Energetics of the structure of the four-α-helix bundle in proteins. *Proc. Natl. Acad. Sci. USA.* 85:4295–4299.

Coles, M., W. Bicknell, A. A. Watson, D. P. Fairlie, and D. J. Craik. 1998. Solution structure of amyloid β-peptide (1–40) in a water-micelle environment. Is the membrane-spanning domain where we think it is? *Biochemistry.* 37:11064–11077.

Cooper, J. H. 1974. Selective amyloid staining as a function of amyloid composition and structure. Histochemical analysis of the alkaline Congo red, standardized toluidine blue, and iodine methods. *Lab. Invest.* 31: 232–238.

Cornell, W. D., P. Cieplak, C. I. Bayly, I. R. Gould, K. M. Merz, D. M. Ferguson, D. C. Spellmeyer, T. Fox, J. W. Caldwell, and P. A. Kollman. 1995. A second generation force field for the simulation of proteins, nucleic acids, and organic molecules. *J. Am. Chem. Soc.* 117: 5179–5197.

Darden, T., D. York, and L. Pedersen. 1993. Particle mesh Ewald: an $N\cdot\log(N)$ method for Ewald sums. *J. Chem. Phys.* 98:10089–10092.

DeLellis, R. A., G. G. Glenner, and J. S. Ram. 1968. Histochemical observations on amyloid with reference to polarization microscopy. *J. Histochem. Cytochem.* 16:663–665.

Dill, K. A. 1990. Dominant forces in protein folding. *Biochemistry.* 29: 7133–7155.

Fraser, P. E., J. T. Nguyen, W. K. Surewicz, and D. A. Kirschner. 1991. pH-dependent structural transitions of Alzheimer amyloid peptides. *Biophys. J.* 60:1190–1201.

Glenner, G. G., and C. W. Wong. 1984. Alzheimer's disease: initial report of the purification and characterization of a novel cerebrovascular amyloid protein. *Biochem. Biophys. Res. Commun.* 120:885–890.

Hamaguchi, N., P. Charifson, T. Darden, L. Xiao, K. Pamanabhan, A. Tulinsky, R. Hiskey, and L. Pedersen. 1992. Molecular dynamics simulations of bovine prothrombin fragment 1 in the presence of calcium ions. *Biochemistry.* 31:8840–8848.

Harper, J. D., C. M. Lieber, and P. T. Lansbury, Jr. 1997. Atomic force microscopic imaging of seeded fibril formation and fibril branching by the Alzheimer's disease amyloid-β protein. *Chem. Biol.* 4:951–959.

Hilbich, C., B. Kisters-Woike, J. Reed, C. L. Masters, and K. Beyreuther. 1991. Aggregration and secondary structure of synthetic amyloid β-A4 peptides of Alzheimer's disease. *J. Mol. Biol.* 218:149–163.

Inouye, H., P. E. Fraser, and D. A. Kirschner. 1993. Structure of β-crystallite assemblies formed by Alzheimer β-amyloid protein analogues: analysis by x-ray diffraction. *Biophys. J.* 64:502–519.

Jarrett, J. T., E. P. Berger, and P. T. Lansbury, Jr. 1993. The carboxy terminus of the β-amyloid protein is critical for the seeding of amyloid formation: implications for the pathogensis of Alzheimer's disease. *Biochemistry.* 32:4693–4698.

Kang, J., H. G. Lemaire, A. Unterbeck, J. M. Salbaum, C. L. Masters, K. H. Grzeschik, G. Multhaup, K. Beyreuther, and B. Muller-Hill. 1987. The precursor of Alzheimer's disease amyloid A4 protein resembles a cell-surface receptor. *Nature.* 325:733–736.

Kelly, J. W. 1998. The alternative conformations of amyloidogenic proteins and their multi-step assembly pathways. *Curr. Opin. Struct. Biol.* 8:101–106.

Kirschner, D. A., H. Inouye, L. K. Duffy, A. Sinclair, M. Lind, and D. J. Selkoe. 1987. Synthetic peptide homologous to β-protein from Alzheimer disease forms amyloid-like fibrils in vitro. *Proc. Natl. Acad. Sci. USA.* 84:6953–8957.

Klunk, W. E., J. W. Pettegrew, and D. J. Abraham. 1989. Two simple methods for quantifying low-affinity dye-substrate binding. *J. Histochem. Cytochem.* 37:1293–1297.

Kusumoto, Y., A. Lomakin, D. B. Teplow, and G. B. Benedek. 1998. Temperature dependence of amyloid β-protein fibrillization. *Proc. Natl. Acad. Sci. USA.* 95:12277–12282.

Langosch, D., and J. Heringa. 1998. Interaction of transmembrane helices by a knobs-into-holes packing characteristic of soluble coiled coils. *Proteins.* 3:150–159 .

Lansbury, P. T., Jr. 1992. In pursuit of the molecular structure of amyloid plaque: new technology provides unexpected and critical information. *Biochemistry.* 31:6865–6870.

Lansbury, P. T., Jr., P. R. Costa, J. M. Griffiths, E. J. Simon, M. Auger, K. J. Halverson, D. A. Kocisko, Z. S. Hendsch, T. T. Ashburn, R. G. Spencer, B. Tidor, and R. G. Griffin. 1995. Structural model for the β-amyloid fibril based on interstrand alignment of an antiparallel-sheet comprising a C-terminal peptide. *Nature Struct. Biol.* 2:990–998.

Lazo, N. D., and D. T. Downing. 1998. Amyloid fibrils may be assembled from β-helical protofibrils. *Biochemistry.* 37:1731–1735.

Lee, J. P., E. R. Stimson, J. R. Ghilardi, P. W. Mantyh, Y. A. Lu, A. M. Felix, W. Llanos, A. Behbin, M. Cummings, M. Van Criekinge, W. Timms, and J. E. Maggio. 1995. ^{1}H NMR of Aβ amyloid peptide congeners in water solution. Conformational changes correlate with plaque competence. *Biochemistry.* 34:5191–5200.

Li, L., T. A. Darden, S. J. Freedman, B. C. Furie, B. Furie, J. D. Baleja, H. Smith, R. G. Hiskey, and L. G. Pedersen. 1997. Refinement of the NMR solution structure of the γ-carboxyglutamic acid domain of coagulation factor IX using molecular dynamics simulation with initial Ca^{2+} positions determined by a genetic algorithm. *Biochemistry.* 36:2132–2138.

Lomakin, A., D. S. Chung, G. B. Benedek, D. A. Kirschner, and D. B. Teplow. 1996. On the nucleation and growth of amyloid β-protein fibrils: detection of nuclei and quantitation of rate constants. *Proc. Natl. Acad. Sci. USA.* 93:1125–1129.

Lorenzo, A., and B. A. Yankner. 1994. β-amyloid neurotoxicity requires fibril formation and is inhibited by Congo red. *Proc. Natl. Acad. Sci. USA.* 91:12243–12247.

Mager, P. P. 1998. Molecular simulation of the primary and secondary structures of the Aβ (1–42) peptide of Alzheimer's disease. *Med. Res. Rev.* 18:403–430.

Malinchik, S. B., H. Inouye, K. E. Szumowski, and D. A. Kirschner. 1998. Structural analysis of Alzheimer's β (1–40) amyloid: protofilament assembly of tubular fibrils. *Biophys. J.* 74:537–545.

Pauling, L., and R. Corey. 1951. Configuration of polypeptide chains with favored orientation around single bonds: two new pleated sheets. *Proc. Natl. Acad. Sci. USA.* 37:729–739.

Pike, C., M. J. Overman, and C. W. Cotman. 1995. Amino-terminal deletions enhance aggregation of β-amyloid peptides in vitro. *J. Biol. Chem.* 270:23895–23898.

Pike, C. J., A. J. Walencewicz, C. G. Glabe, and C. W. Cotman. 1991. In vitro aging of β-amyloid protein causes peptide aggregation and neurotoxicity. *Brain Res.* 563:311–314.

Pollack, S. J., I. I. Sadler, S. R. Hawtin, V. J. Tailor, and M. S. Shearman. 1995. Sulfonated dyes attenuate the toxic effects of β-amyloid in a structure-specific fashion. *Neurosci. Lett.* 197:211–214.

Puchtler, H., F. Sweat, and M. Levine. 1962. On the binding of Congo red by amyloid. *J. Histochem.* 10:355–364.

Selkoe, D. J. 1996. Amyloid β-protein and the genetics of Alzheimer's disease. *J. Biol. Chem.* 271:18295–18298.

Serpell, L. C., M. Sunde, P. E. Fraser, P. K. Luther, E. P. Morris, O. Sangren, E. Lundgren, and C. C. F. Blake. 1995. Examination of the structure of the transthyretin amyloid fibril by image reconstruction from electron micrographs. *J. Mol. Biol.* 254:113–118.

Simmons, L. K., P. C. May, K. J. Tomaselli, R. E. Rydel, K. S. Fuson, E. F. Brigham, S. Wright, I. Lieberburg, G. W. Becker, D. N. Brems, and W. Y. Li. 1994. Secondary structure of amyloid β-peptide correlates with neurotoxic activity in vitro. *Mol. Pharmacol.* 45:373–379.

Snow, A. D., R. Sekiguchi, D. Nochlin, P. Fraser, K. Kimata, A. Mizutani, M. Arai, W. A. Schreier, and D. G. Morgan. 1994. An important role of heparan sulfate proteoglycan (Perlecan) in a model system for the deposition and persistence of fibrillar A β-amyloid in rat brain. *Neuron.* 12:219–234.

Sticht, H., P. Bayer, D. Willbold, S. Dames, C. Hilbich, K. Beyreuther, R. W. Frank, and P. Rösch. 1995. Structure of amyloid A4–1(1–40)-peptide of Alzheimer's disease. *Eur. J. Biochem.* 233:293–298.

Sunde, M., L. C. Serpell, M. Bartlam, P. E. Fraser, M. B. Pepys, and C. C. F. Blake. 1997. Common core structure of amyloid fibrils by synchrotron x-ray diffraction. *J. Mol. Biol.* 273:729–739.

Tjernberg, L. O., J. Naslund, F. Lindqvist, J. Johansson, A. R. Karlstrom, J. Thyberg, L. Terenius, and C. Nordstedt. 1996. Arrest of β-amyloid formation by a pentapeptide ligand. *J. Biol. Chem.* 271:8545–8548.

Turnell, W. G., and J. T. Finch. 1992. Binding of the dye Congo red to the amyloid protein pig insulin reveals a novel homology amongst amyloid-forming peptide sequences. *J. Mol. Biol.* 20:1205–1223.

Walsh, D. M., A. Lomakin, G. B. Benedek, M. M. Condron, and D. B. Teplow. 1997. Amyloid β-protein fibrillogenesis. Detection of a protofibrillar intermediate. *J. Biol. Chem.* 272:22364–22372.

Wood, S. J., R. Wetzel, J. D. Martin, and M. R. Hurle. 1995. Prolines and amyloidogenicity in fragments of the Alzheimer's peptide β/A4. *Biochemistry.* 34:724–730.